International Journal of
Molecular Sciences

MDPI

Article

Effect of the Interaction between Elevated Carbon Dioxide and Iron Limitation on Proteomic Profiling of Soybean

José C. Soares [1], Hugo Osório [2,3], Manuela Pintado [1] and Marta W. Vasconcelos [1,*]

[1] CBQF—Centro de Biotecnologia e Química Fina—Laboratório Associado, Escola Superior de Biotecnologia, Universidade Católica Portuguesa, Rua Diogo Botelho 1327, 4169-005 Porto, Portugal
[2] i3S—Instituto de Investigação e Inovação em Saúde, Universidade do Porto, 4200-135 Porto, Portugal
[3] Ipatimup—Institute of Molecular Pathology and Immunology of the University of Porto, University of Porto, 4200-135 Porto, Portugal
* Correspondence: mvasconcelos@ucp.pt

Abstract: Elevated atmospheric CO_2 (eCO_2) and iron (Fe) availability are important factors affecting plant growth that may impact the proteomic profile of crop plants. In this study, soybean plants treated under Fe-limited (0.5 mM) and Fe-sufficient (20 mM) conditions were grown at ambient (400 µmol mol^{-1}) and eCO_2 (800 µmol mol^{-1}) in hydroponic solutions. Elevated CO_2 increased biomass from 2.14 to 3.14 g $plant^{-1}$ and from 1.18 to 2.91 g $plant^{-1}$ under Fe-sufficient and Fe-limited conditions, respectively, but did not affect leaf photosynthesis. Sugar concentration increased from 10.92 to 26.17 µmol g FW^{-1} in roots of Fe-sufficient plants and from 8.75 to 19.89 µmol g FW^{-1} of Fe-limited plants after exposure to eCO_2. In leaves, sugar concentration increased from 33.62 to 52.22 µmol g FW^{-1} and from 34.80 to 46.70 µmol g FW^{-1} in Fe-sufficient and Fe-limited conditions, respectively, under eCO_2. However, Fe-limitation decreases photosynthesis and biomass. Pathway enrichment analysis showed that cell wall organization, glutathione metabolism, photosynthesis, stress-related proteins, and biosynthesis of secondary compounds changed in root tissues to cope with Fe-stress. Moreover, under eCO_2, at sufficient or limited Fe supply, it was shown an increase in the abundance of proteins involved in glycolysis, starch and sucrose metabolism, biosynthesis of plant hormones gibberellins, and decreased levels of protein biosynthesis. Our results revealed that proteins and metabolic pathways related to Fe-limitation changed the effects of eCO_2 and negatively impacted soybean production.

Keywords: elevated CO_2; iron limitation; soybean; proteomic profiling

Citation: Soares, J.C.; Osório, H.; Pintado, M.; Vasconcelos, M.W. Effect of the Interaction between Elevated Carbon Dioxide and Iron Limitation on Proteomic Profiling of Soybean. *Int. J. Mol. Sci.* **2022**, *23*, 13632. https://doi.org/10.3390/ijms232113632

Academic Editors: Stefania Astolfi and Silvia Celletti

Received: 5 October 2022
Accepted: 4 November 2022
Published: 7 November 2022

1. Introduction

Atmospheric carbon dioxide (CO_2) concentrations are projected to increase to at least 700–1000 µmol mol^{-1} at the end of this century [1]. The trend in crop responses under elevated CO_2 (eCO_2) is supposed to have a noticeable influence on the global food chain and may threaten human nutrition [2]. The impact of eCO_2 varies among different crop species, but eCO_2 generally improves the photosynthesis of the C3 plants [3] by repressing the oxygenase activity of ribulose-1,5-bisphosphate and by improving carbon assimilation used for plant growth [4]. Nevertheless, plant-based responses to eCO_2 are affected by nutrient bioavailability, including iron (Fe) [5]. Iron is considered a limiting factor and plays a key role in biomass production and seed yield in crops including tomato [5], spinach [6], potato, and rice [7]. The mineral element is of particular significance because of its role in photosynthetic CO_2 fixation, which utilizes Fe as a crucial element to ensure photosynthetic efficiency [4]. Anyway, Fe is the most frequently deficient micronutrient in the human diet, affecting an estimated 2 billion people [8]. While eCO_2 promotes plant growth, the interaction with Fe-limitation has not been well documented. Due to the increase in plant growth, the plant requirement for nutrients also increases, and the restriction of macro and micronutrient content at eCO_2 generally inhibits the increase in

plant biomass [4]. Accordingly, low nitrate supply limits shoot growth and hormonal responses to eCO_2 [2], involving alterations in protein synthesis and metabolic pathways associated with eCO_2 and nitrate. The proteomic analysis demonstrated an increase in the expression of many proteins due to eCO_2 under adequate nitrate levels involved with cell cycle and proliferation, transcription and translation, photosynthesis, amino acids synthesis, sucrose, and starch metabolism, and ABA signaling pathways. Proteomic analysis showed that eCO_2 affected various metabolic processes and pathways, such as photosynthetic carbon fixation, respiratory metabolism, cellular growth, and stress defense [9,10]. Yu et al. [11] also demonstrated that eCO_2 improved heat tolerance in bermudagrass attributed to metabolic pathways during which proteins and metabolites were upregulated, including light reaction and carbon fixation of photosynthesis, glycolysis and TCA cycle, and amino acid metabolism.

Iron is an essential micronutrient that impacts plant productivity, and its bioavailability to plants is often limited in calcareous soils [12], which account for ~30% of the world's agricultural soil. In tomato plants grown in Fe-limited and Fe-sufficient conditions, eCO_2 increased plant biomass and root-to-shoot ratio compared to plants grown in ambient CO_2 (aCO_2) conditions. The percentage increase in biomass was higher in Fe-limited plants compared to Fe-sufficient plants. Therefore, shoot fresh weight increased under eCO_2 conditions by 22% and 44% in Fe-sufficient and Fe-limited conditions, respectively, and fresh root weight by 43% and 97% [5]. Likewise, eCO_2 induced biomass production in barley grown at Fe-sufficient and Fe-deficient conditions and increased shoot Fe concentration and Fe-acquisition mechanisms in Fe-deficient plants, indicating an improved internal Fe utilization [13]. The proteomic characterization of Fe deficiency responses in cucumber roots revealed that most of the increased proteins belong to glycolysis and nitrogen metabolism, and proteins with low expression levels were related to the metabolism of sucrose, structural carbohydrates, and proteins [14]. In addition, proteins associated with stress adaptation, reactive oxygen species-related proteins, and mitochondrial proteins were differentially expressed under long-term Fe-restriction on the roots of different pea cultivars [15]. López-Millán et al. [16] revealed some common elements in proteome under Fe-limitation involving several plant species. Oxidative stress and defense-related proteins, C and N metabolism-related proteins, cell wall proteins, secondary metabolism-associated proteins, energy-related proteins, transport, and protein metabolism have been identified as differentially accumulated proteins among plant species.

Therefore, we consider that it is relevant to discover the complex response mechanisms of soybean plants to future climatic conditions, such as eCO_2 and Fe-limitation. This study aimed to understand how soybean plants respond to eCO_2, Fe-stress, and their combination at the level of plant growth, carbohydrate content, photosynthesis, and the expression profile of the leaf and root proteome. At the same time, it was our purpose to investigate if eCO_2 can mitigate the adverse effects of Fe-limitation in soybean plants and provide several insights into improving stress tolerance in the future environment.

2. Results

2.1. Interactive Effects of eCO_2 and Fe-Limitation on Plant Biomass

Both eCO_2 and Fe-limitation showed significant effects ($p < 0.05$) on plant biomass with a significant CO_2 x Fe interaction (Table 1). Elevated CO_2 increased plant dry weight from 2.14 to 3.14 g plant^{-1} under Fe-sufficient conditions and from 1.18 to 2.91 g plant^{-1} under Fe-limited conditions. Furthermore, Fe-limitation significantly decreased plant biomass at aCO_2 ($p < 0.05$) but not at eCO_2 ($p > 0.05$).

Table 1. Effects of eCO_2 and Fe-limitation on biomass, sugar content, and gas exchange parameters in soybean plants.

	Treatments				Two-Way ANOVA			
Measurements	**Fe+ELE**	**Fe+AMB**	**Fe-ELE**	**Fe-AMB**	**d.f.**	**CO_2**	**Fe**	**CO_2 × Fe**
Total biomass (g plant^{-1})	3.14 ± 0.19 ^{a}	2.14 ± 0.15 ^{b}	2.91 ± 0.12 ^{a}	1.18 ± 0.08 ^{c}	1	**94.29; <0.001**	**18.04; <0.001**	**6.59; 0.021**
Pn (μmol m^{-2} s^{-1})	11.21 ± 0.43 ^{a}	11.43 ± 0.55 ^{a}	9.21 ± 0.40 ^{b}	8.90 ± 0.80 ^{b}	1	0.006; 0.939	**15.17; <0.001**	0.21; 0.654
gs (mol m^{-2} s^{-1})	0.13 ± 0.01 ^{a}	0.37 ± 0.03 ^{b}	0.12 ± 0.01 ^{a}	0.30 ± 0.02 ^{c}	1	**85.74; <0.001**	**6.568; 0.021**	**5.42; 0.033**
Tr (mol m^{-2} s^{-1})	2.46 ± 0.19 ^{a}	5.22 ± 0.36 ^{b}	2.28 ± 0.16 ^{a}	4.13 ± 0.29 ^{d}	1	**54.19; <0.001**	3.84; 0.068	4.44; 0.051
Sugar (roots, μmol g FW^{-1})	26.17 ± 3.72 ^{a}	10.92 ± 1.12 ^{b}	19.89 ± 2.36 ^{c}	8.75 ± 0.92 ^{b}	1	**9.90; 0.009**	4.82; 0.051	1.85; 0.201
Sugar (leaves, μmol g FW^{-1})	52.22 ± 4.03 ^{a}	33.62 ± 1.21 ^{b}	46.70 ± 2.54 ^{a}	34.80 ± 2.44 ^{b}	1	**37.71; <0.001**	0.761; 0.406	1.82; 0.210

Note: Fe+AMB, Fe-sufficient + aCO_2; Fe+ELE, Fe-sufficient + eCO_2; Fe-AMB, Fe-limitation + aCO_2; Fe-ELE, Fe-limitation + eCO_2; Data are mean ± SE (n = 5). Different lowercase superscript letters in the same row indicate the significant difference at $p < 0.05$ level. CO_2, Fe, and CO_2 × Fe indicate CO_2 treatment, Fe treatment, and the interaction of CO_2 by Fe treatment, respectively. Results from the analysis of variance with degrees of freedom (d.f.), F ratios, and probabilities (p) for some parameters. Significant effects are shown in boldface.

2.2. Interactive Effects of eCO_2 and Fe-Limitation on Photosynthesis Parameters

Fe-limitation showed a significant effect on Pn ($p < 0.05$), whereas at eCO_2 ($p > 0.05$, Table 1), a significant effect was not detected. The decrease in Pn due to Fe-limitation was −21.7% and −28.4% under eCO_2 and aCO_2 conditions, respectively. Elevated CO_2 significantly decreased gs under both Fe supplies ($p < 0.05$). Moreover, under Fe-limitation, gs was reduced at aCO_2 ($p < 0.05$) and at eCO_2 conditions ($p > 0.05$). The transpiration rate (Tr) was decreased by eCO_2 ($p < 0.05$) and by Fe-stress at aCO_2 conditions ($p < 0.05$).

2.3. Interactive Effects of eCO_2 and Fe-Limitation on Sugar Content

Elevated CO_2 showed a significant effect on sugar concentration in the root ($p < 0.05$, Table 1) and leaf tissues ($p < 0.05$) but was not affected by Fe-limitation ($p > 0.05$). Sugar concentration increased from 10.92 to 26.17 μmol g FW^{-1} in the roots of Fe-sufficient plants and from 8.75 to 19.89 μmol g FW^{-1} in the roots of Fe-limited plants after exposure to eCO_2. In leaves, sugar concentration increased from 33.62 to 52.22 μmol g FW^{-1} in Fe-sufficient conditions and from 34.80 to 46.70 μmol g FW^{-1} in Fe-limited conditions.

2.4. Functional Categories of Differentially Expressed Proteins

Tables S1 and S2 go into depth about the entire list of proteins that were found and measured. Proteins with a p-value below 0.05 and a fold change ratio above 1.2 or below 1/1.2 were considered as DEPs (Figure 1 and Tables S3 and S4).

Among the identified proteins, 705 were differentially expressed in root tissues considering a fold change ratio of above 1.2 or below 1/1.2 ($p < 0.05$, Figure 1A). We found 27 and 136 proteins that were upregulated under eCO_2 (Fe+ELE/Fe+AMB) and Fe-limitation (Fe-AMB/Fe+AMB), respectively, with an overlap of one protein (Fe2OG dioxygenase domain-containing protein, Figure S1). Furthermore, 167 and 110 proteins were downregulated by eCO_2 and Fe-limitation, respectively, with an overlap of two HMA domain-containing proteins, one superoxide dismutase and one 2-isopropylmalate synthase. Compared to control plants, 141 proteins were up and 79 downregulated by the interaction of eCO_2 with Fe-limitation (Fe-ELE/Fe+AMB). We also found 139 up and 119 downregulated proteins in Fe-ELE/Fe-AMB conditions. Protein expression profiles could be correctly distinguished between treatments using the heat map of differentially expressed proteins (Figure 1B). The metabolism overview maps showed changes at the protein level obtained using the MapMan software. Proteins associated with redox regulation and cell wall metabolism decreased the expression levels under eCO_2, and photosynthetic light reactions proteins were upregulated by Fe-limitation, as shown in Figure 2.

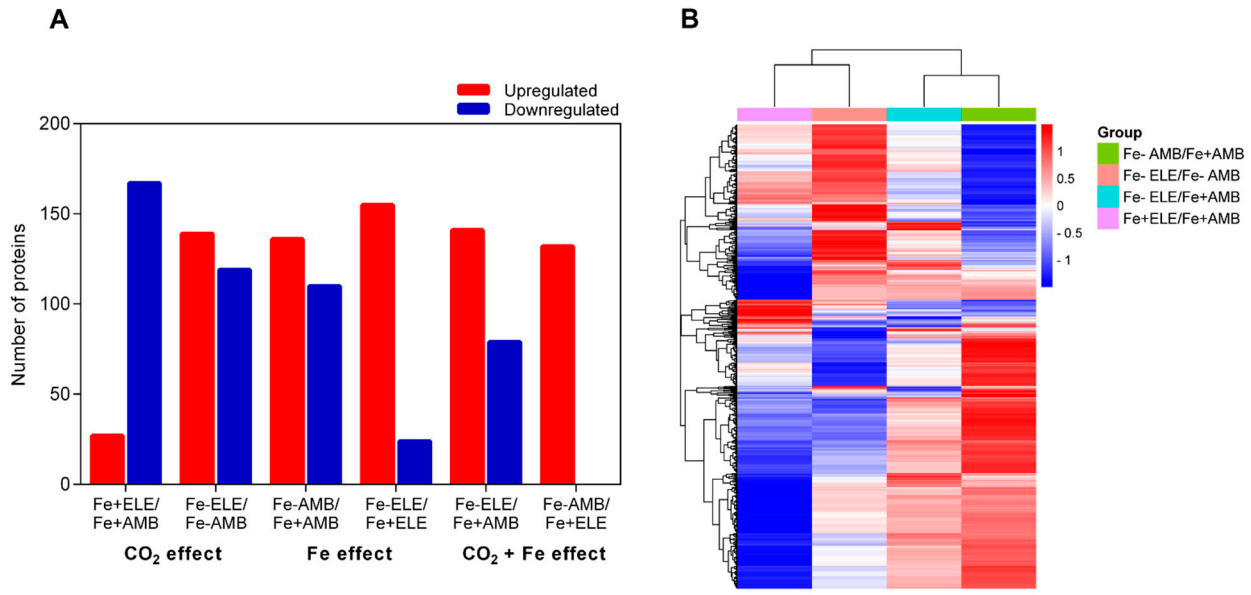

Figure 1. Soybean root proteome profiles under eCO_2 and Fe-limitation. (**A**) The number of up-regulated and downregulated proteins in soybean root in response to eCO_2 and Fe-limitation; (**B**) Cluster analysis of all differently regulated proteins among different treatments. Fe+AMB, Fe-sufficient + aCO_2; Fe+ELE, Fe-sufficient + eCO_2; Fe-AMB, Fe-limitation + aCO_2; Fe-ELE, Fe-limitation + eCO_2.

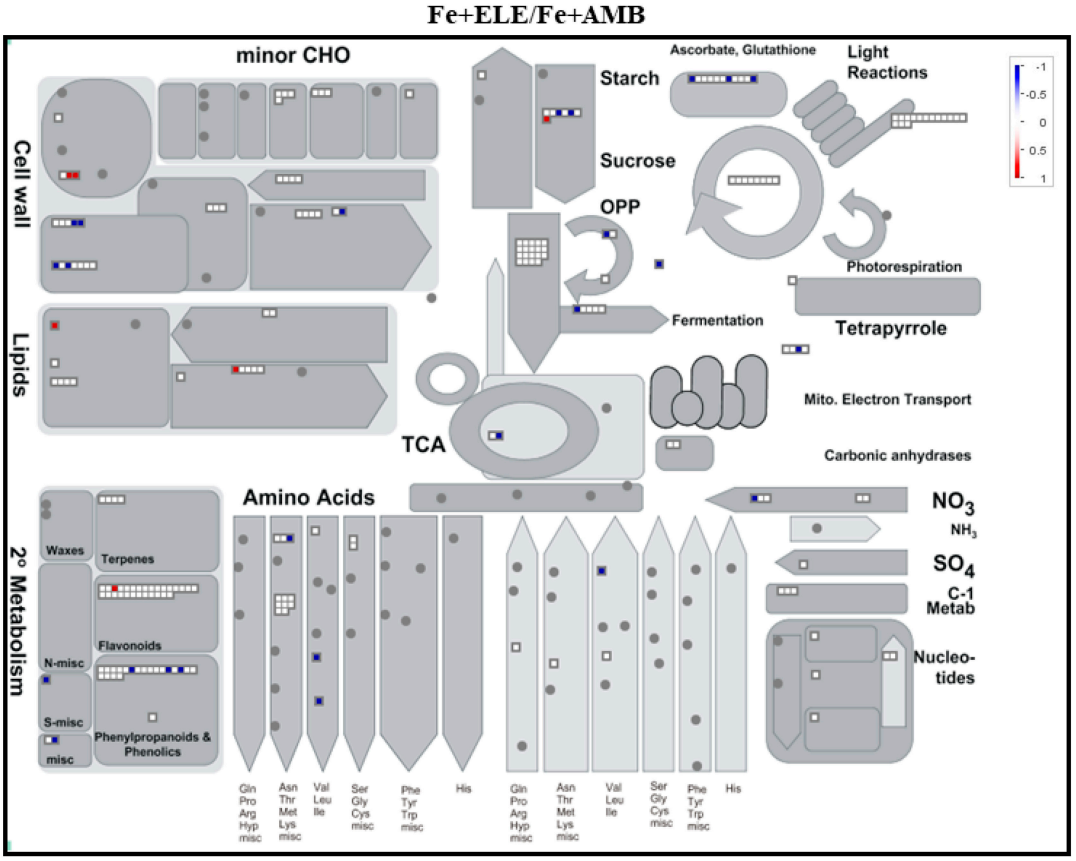

Figure 2. *Cont.*

Fe-ELE/Fe-AMB

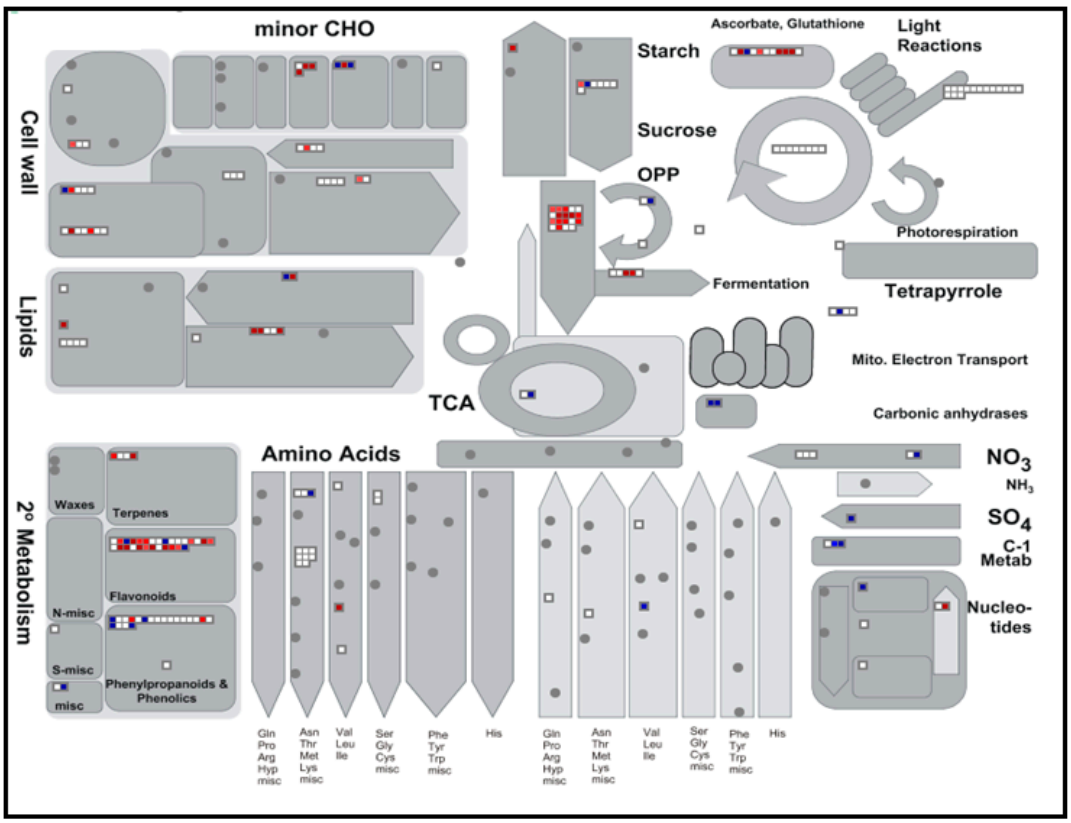

Fe-AMB/Fe+AMB

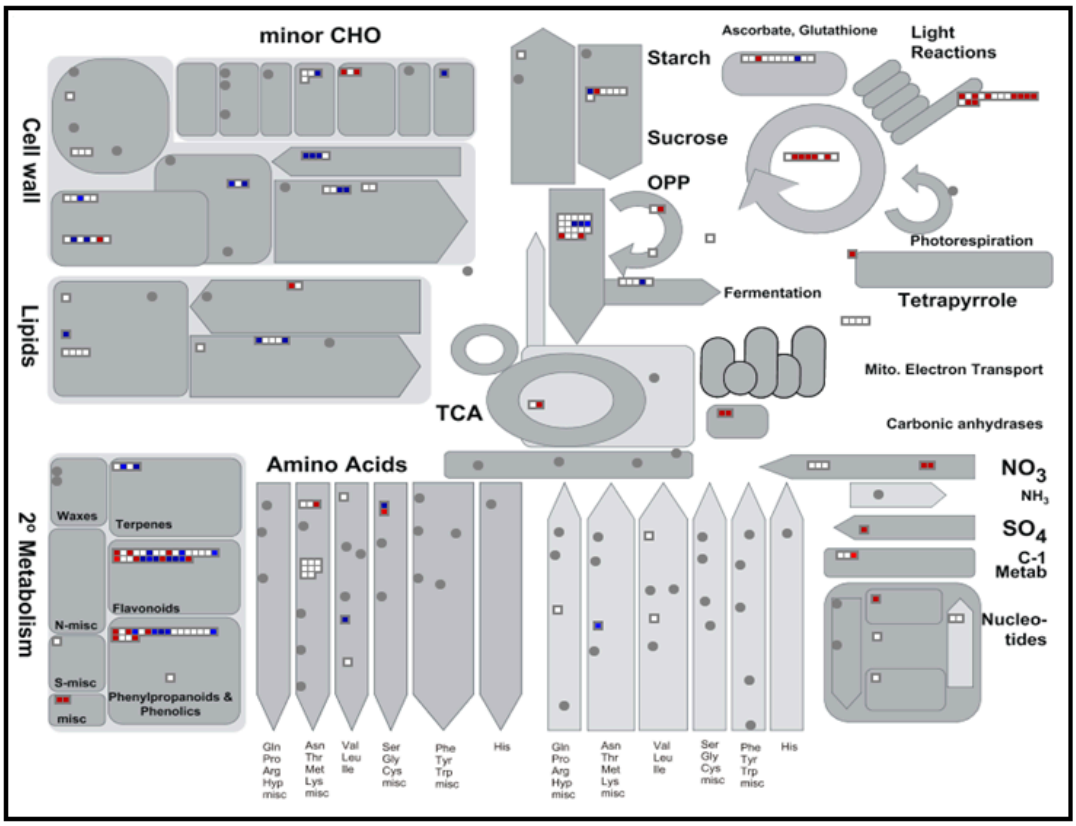

Figure 2. *Cont.*

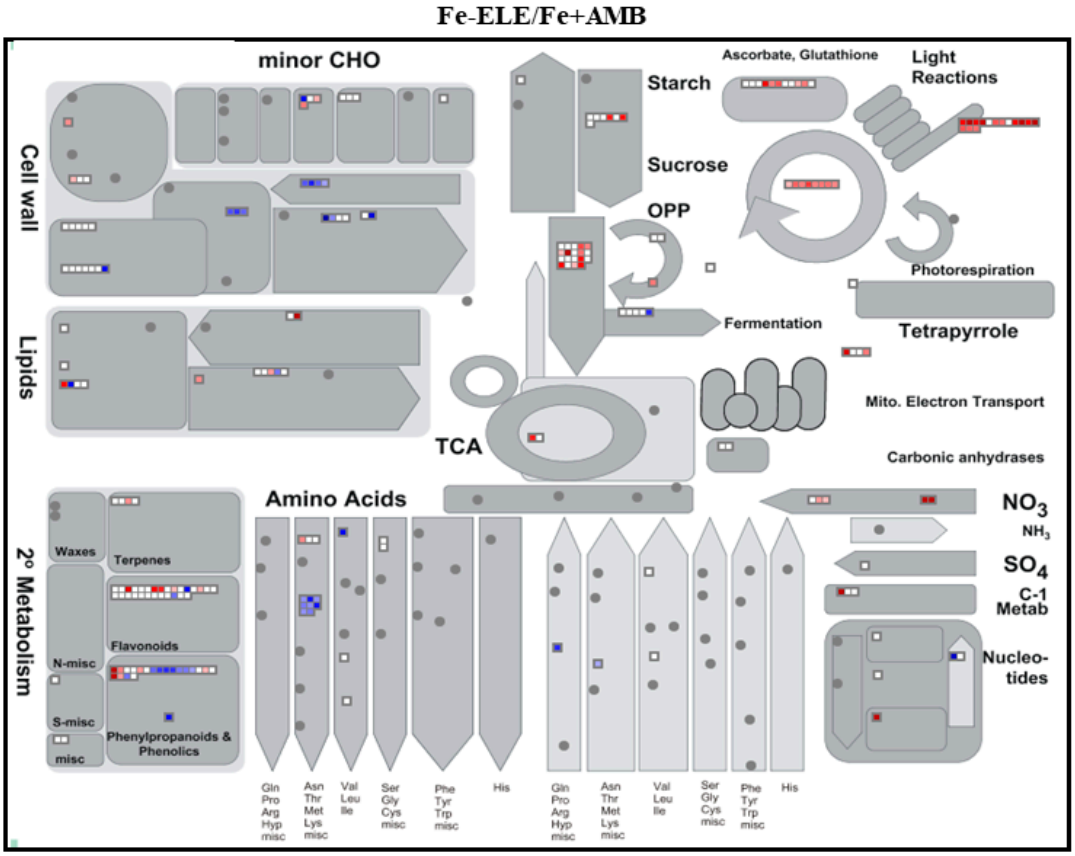

Figure 2. MapMan metabolism overview maps showing changes in DEPs in root tissues under eCO_2 and Fe-limitation. Fe+AMB, Fe-sufficient + aCO_2; Fe+ELE, Fe-sufficient + eCO_2; Fe-AMB, Fe-limitation + aCO_2; Fe-ELE, Fe-limitation + eCO_2. Boxes represent log2 expression values, genes in red are upregulated, and those in blue are repressed.

In addition, proteins related to photosynthetic light reactions, glycolysis, and redox regulation were upregulated in Fe-ELE/Fe+AMB conditions. Enzymes associated with secondary metabolism, glycolysis, and redox regulation were upregulated in Fe-ELE/Fe-AMB conditions. The number of differentially regulated proteins, according to functional categories and cellular localization, is summarized in Figure 3.

Most enzymes in root tissues with assigned functions were "protein-related," "stress-related," "secondary metabolism-related," and "RNA-related," and were mostly downregulated in response to eCO_2. Protein synthesis, photosynthesis-related, and redox-related enzymes were mainly upregulated under Fe-limited conditions. In Fe-ELE/Fe+AMB conditions, most proteins were associated with photosynthesis, hormone metabolism, redox regulation, signaling, and glycolysis and upregulated. In addition, most enzymes related to protein synthesis were downregulated, and enzymes associated with secondary metabolism, hormone metabolism, stress, and glycolysis were upregulated in the Fe-ELE treatment compared with Fe-AMB. According to their cellular location, most proteins identified were in the cytosol, followed by the extracellular space and nucleus.

In leaves, a total of 589 proteins were differentially expressed (fold change ratio > 1.2 or <1/1.2 and $p < 0.05$). As shown in Figure 4, the gene expression profile between treatments could be distinguished and included 72 and 101 proteins that were up and downregulated, respectively, under eCO_2.

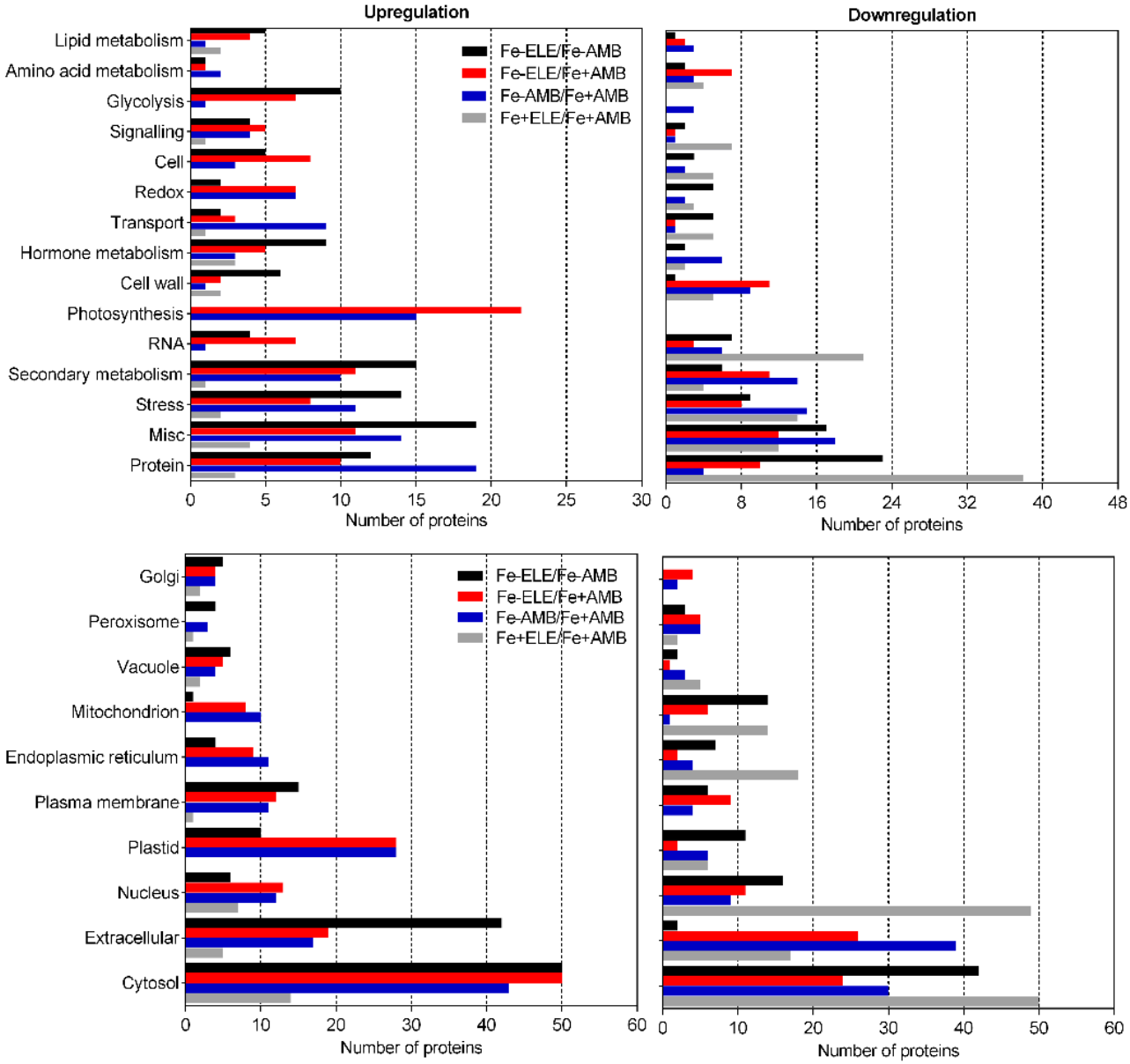

Figure 3. Numbers of DEPs identified from soybean roots at different CO_2 levels under sufficient and limited Fe-supply according to functional categories and subcellular compartments by MapMan. Fe+AMB, Fe-sufficient + aCO_2; Fe+ELE, Fe-sufficient + eCO_2; Fe-AMB, Fe-limitation + aCO_2; Fe-ELE, Fe-limitation + eCO_2.

However, Fe-limitation resulted in 146 up and 104 downregulated proteins. In upregulated, an overlap of 14 proteins (Figure S2), whereas, in downregulated proteins, an overlap of 27 proteins was observed between eCO_2 and Fe-limitation. The interaction of Fe-limitation and eCO_2 resulted in 83 and 76 proteins being upregulated and downregulated, respectively. From the upregulated proteins, the interaction induced an overlap of 28 proteins with Fe-limitation or 27 proteins with eCO_2. Regarding downregulated proteins, plants grown under Fe-limitation and eCO_2 had an overlap of 41 proteins with Fe-stress and 36 proteins with eCO_2. Furthermore, 74 and 136 proteins were upregulated and downregulated in the Fe-ELE/Fe-AMB conditions. Figure 5 displays the metabolism overview maps in the leaf tissues, and eCO_2 increased the expression of enzymes involved in glycolysis, photosynthesis, and redox homeostasis, while Fe-limitation decreased the expression of proteins involved in photosynthetic light processes.

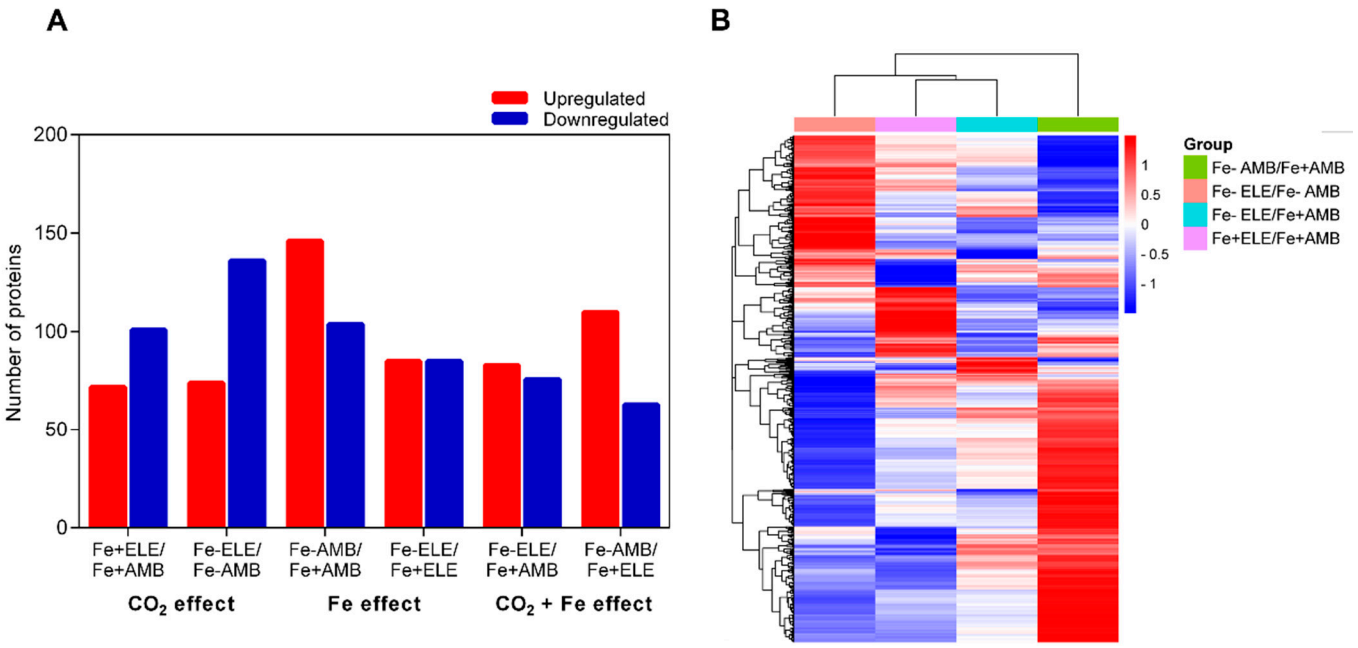

Figure 4. Soybean leaf proteome profiles under eCO_2 and Fe-limitation. (**A**) The number of upregulated and downregulated proteins in soybean leaf in response to eCO_2 and Fe-limitation; (**B**) Cluster analysis of all differently regulated proteins among different treatments. Fe+AMB, Fe-sufficient + aCO_2; Fe+ELE, Fe-sufficient + eCO_2; Fe-AMB, Fe-limitation + aCO_2; Fe-ELE, Fe-limitation + eCO_2.

In Fe-ELE/Fe+AMB conditions, the expression of proteins involved in glycolysis and redox homeostasis increased. However, in Fe-ELE/Fe-AMB, enzymes related to glycolysis and carbohydrate metabolism were increased. The number of DEPs, according to functional categories and cellular compartments, is described in Figure 6. Elevated CO_2 increases the proteins involved in stress, photosynthesis, and glycolysis while downregulating the enzymes involved in signaling and protein synthesis. Furthermore, protein synthesis and secondary metabolism-related proteins exhibited high expression levels, while photosynthesis-related proteins had low levels under Fe-limitation. Most glycolysis-related proteins were downregulated in Fe-ELE/Fe+AMB. In addition, most proteins associated with carbohydrate metabolism, photosynthesis, stress, and glycolysis were upregulated, and protein synthesis-related enzymes were downregulated in Fe-ELE compared with Fe-AMB. Concerning their cellular location, most of the proteins identified were in the cytosol, followed by the plastid and extracellular space (Figure 6).

2.5. Metabolic Pathways Related to the Interaction of eCO_2 and Fe-Limitation

To gain a better understanding of the DEPs between different treatments, pathway enrichment analysis was conducted and shown in Tables 2 and 3. The photosynthesis-related pathways (bin 1) were upregulated in the Fe-AMB vs. Fe+AMB and Fe-ELE vs. Fe+AMB treatments in the root. Glycolysis (bin 4.1) was not affected by eCO_2 and Fe-limitation but was upregulated under Fe-ELE treatment compared to Fe+AMB and Fe-AMB. Cell wall organization (bin 10) and metal binding (bin 15.2) were not affected by eCO_2 but downregulated by Fe-limitation and the interaction of eCO_2 and Fe-limitation. The secondary metabolism (bin 16) was negatively downregulated by Fe-limitation and upregulated by eCO_2 under Fe-limitation (Fe-ELE vs. Fe-AMB). Enzymes involved in hormone metabolism (bin 17.6) had a higher level of expression at eCO_2 under Fe-sufficient and Fe-limited conditions. Proteins associated with stress responses (bins 20.1 and 20.2.1) had low expression under Fe-stress. Moreover, an increase in ascorbate and glutathione metabolism (bin 21.2.1.3), which is an effective mechanism of plant detoxification, was induced by Fe-ELE compared with Fe+AMB conditions. Peroxidases (bin 26.12), phosphatases (bin 26.13), and oxygenases (bin 26.14) were not affected by CO_2 enrichment but downregulated by

Fe-limitation. The expression of glutathione S-transferase proteins (bin 26.9) was higher in Fe-limited plants. Inhibition of gene expression in RNA (bin 27) and protein synthesis (bin 29) pathways occurred under eCO_2.

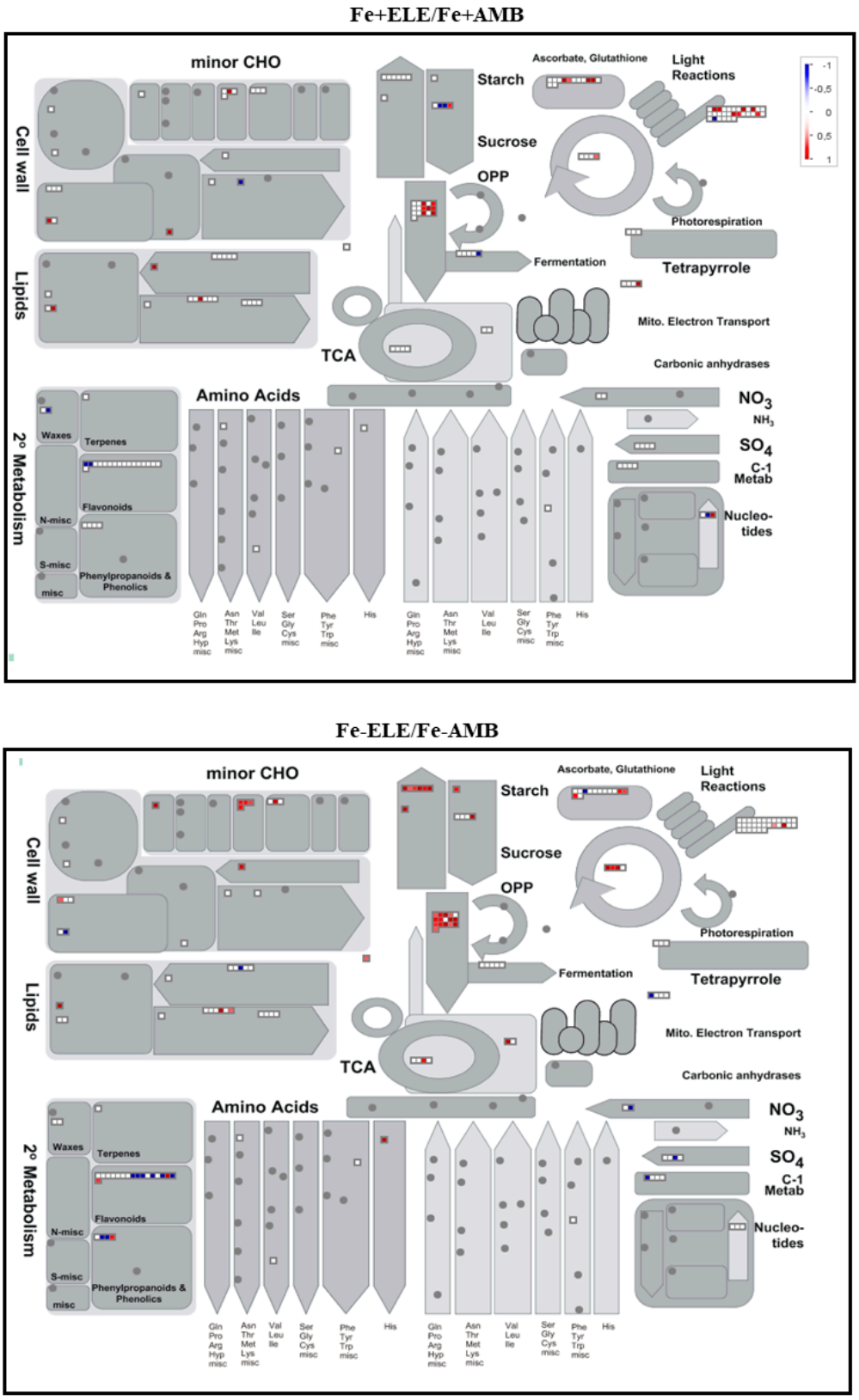

Figure 5. *Cont.*

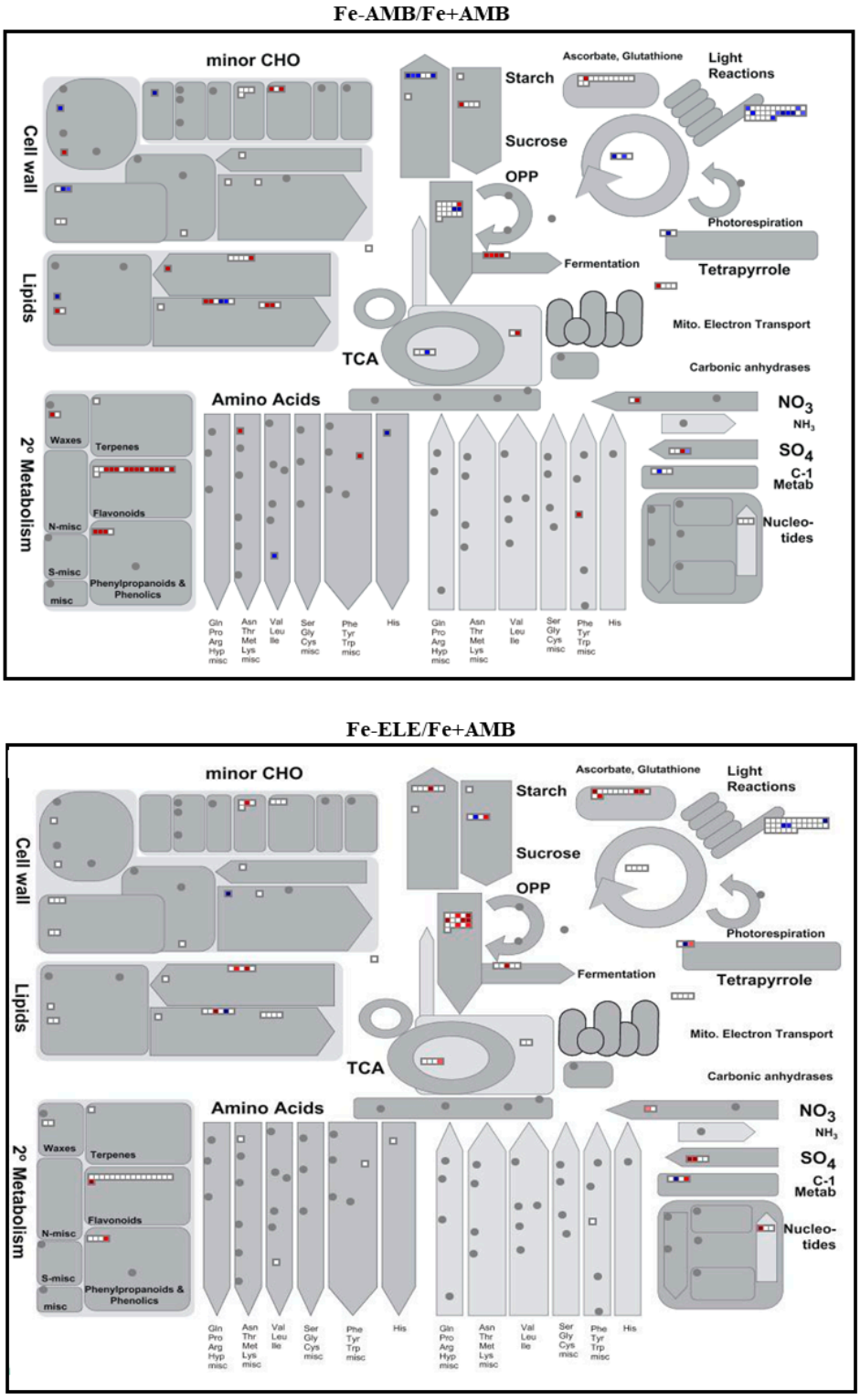

Figure 5. MapMan metabolism overview maps showing changes in DEPs in leaf tissues under eCO_2 and Fe-limitation. Fe+AMB, Fe-sufficient + aCO_2; Fe+ELE, Fe-sufficient + eCO_2; Fe-AMB, Fe-limitation + aCO_2; Fe-ELE, Fe-limitation + eCO_2. Squares represent log2 expression values, and genes in red are upregulated, and those in blue are repressed.

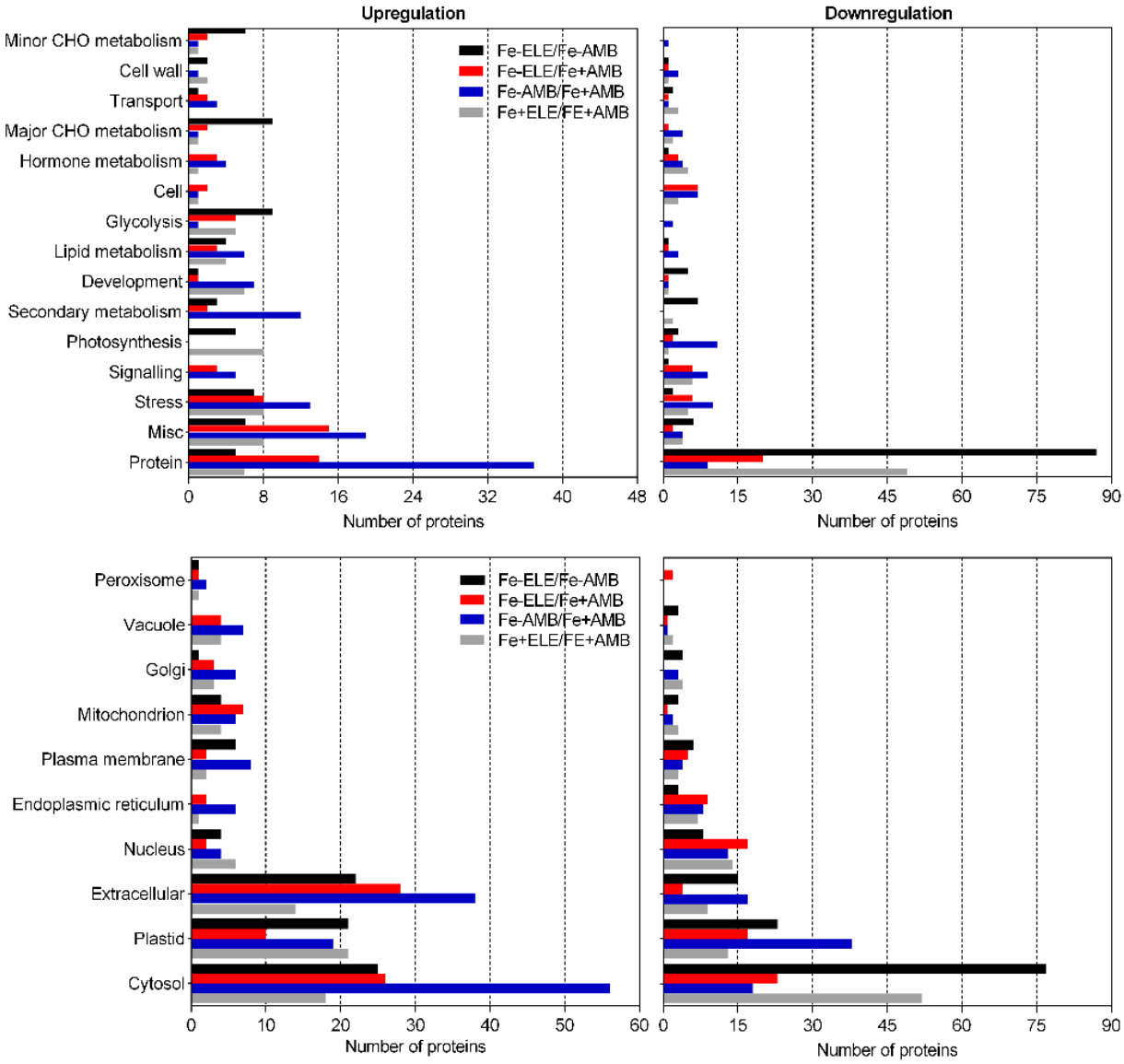

Figure 6. Numbers of DEPs identified from soybean leaves at different CO_2 levels under sufficient and limited Fe-supply according to functional categories and subcellular compartments by MapMan. Fe+AMB, Fe-sufficient + aCO_2; Fe+ELE, Fe-sufficient + eCO_2; Fe-AMB, Fe-limitation + aCO_2; Fe-ELE, Fe-limitation + eCO_2.

Table 2. Pathway enrichment analysis of DEPS in roots of soybean plants under eCO_2 and Fe-limitation.

Bin Code	Bin Name	Fe+ELE vs. Fe+AMB	*p*-Value	Fe-AMB vs. Fe+AMB	*p*-Value	Fe-ELE vs. Fe+AMB	*p*-Value	Fe-ELE vs. Fe-AMB	*p*-Value
1.1.1	PS. Light reaction. Photosystem II	-	-	UP	2.9×10^{-5}	UP	1.7×10^{-5}	-	-
1.1.2	PS. Light reaction. Photosystem I	-	-	UP	1.5×10^{-2}	UP	3.8×10^{-5}	-	-
1.3	PS. Calvin cycle	-	-	-	-	UP	4.4×10^{-4}	-	-
4.1	Glycolysis. Cytosolic branch	-	-	-	-	UP	1.5×10^{-3}	UP	1.7×10^{-2}
10	Cell wall	-	-	DOWN	5.6×10^{-7}	DOWN	1.6×10^{-3}	-	-
13.1.3.4	Amino acid metabolism. Synthesis. Aspartate family. Methionine	-	-	-	-	DOWN	6.9×10^{-3}	-	-

Table 2. *Cont.*

Bin Code	Bin Name	Fe+ELE vs. Fe+AMB	*p*-Value	Fe-AMB vs. Fe+AMB	*p*-Value	Fe-ELE vs. Fe+AMB	*p*-Value	Fe-ELE vs. Fe-AMB	*p*-Value
15.2	Metal handling. Binding, chelation, and storage	-	-	DOWN	3.3×10^{-3}	DOWN	4.3×10^{-7}	-	-
16.1	Secondary metabolism. Isoprenoids	-	-	DOWN	8.3×10^{-3}			UP	1.6×10^{-4}
16.2.1	Secondary metabolism. Phenylpropanoids. Lignin biosynthesis	-	-	DOWN	1.8×10^{-3}	DOWN	2.6×10^{-2}	-	-
16.8	Secondary metabolism. Flavonoids	-	-	DOWN	1.4×10^{-2}	-	-	UP	3.1×10^{-4}
17.6	Hormone metabolism. Gibberellin	UP	1.4×10^{-4}	DOWN	8.3×10^{-3}	-	-	UP	3.6×10^{-4}
20.1	Stress. Biotic	-	-	DOWN	5.6×10^{-3}	-	-	UP	2.1×10^{-3}
20.2.1	Stress. Abiotic. Heat	-	-	DOWN	4.6×10^{-2}	-	-	-	-
21.2.1.3	Redox. Ascorbate and glutathione. Ascorbate. L-galactose-1-phosphate phosphatase	-	-	-	-	UP	2.1×10^{-2}	-	-
26.9	Misc. Glutathione S-transferases	-	-	UP	1.5×10^{-2}	-	-	DOWN	1.3×10^{-3}
26.12	Misc. Peroxidases	-	-	DOWN	2.7×10^{-3}	-	-	UP	1.3×10^{-3}
26.13	Misc. Acid and other phosphatases	-	-	DOWN	6.1×10^{-3}	-	-	UP	3.6×10^{-4}
26.14	Misc. Oxygenase	-	-	DOWN	4.2×10^{-2}	-	-	-	-
27.3	RNA. Regulation of transcription	DOWN	9.4×10^{-3}	-	-	-	-	-	-
27.4	RNA.RNA binding	DOWN	4.4×10^{-2}	-	-	-	-	-	-
29.2.1	Protein. Synthesis. Ribosomal protein	DOWN	4.2×10^{-2}	UP	2.9×10^{-5}	-	-	DOWN	1.0×10^{-14}
34	Transport	-	-	UP	3.1×10^{-2}	-	-	DOWN	3.7×10^{-2}

The expression levels of transport proteins (bin 34) involved in the translocation of solutes across membranes were not affected by eCO_2. Regarding leaf tissues, listed photosynthesis (bin 1) associated pathways were downregulated by Fe-stress. Upregulation of sucrose and starch biosynthesis (bin 2.1) genes occurred at eCO2 under Fe-limited conditions, while downregulation was noticeable in low-Fe supply. Furthermore, glycolysis (bin 4.1) involved in the breakdown of sugars was upregulated by eCO_2 under Fe-limited and Fe-sufficient conditions and not affected by Fe-stress. Stimulation of fatty acid degradation was apparent by eCO2 under Fe-limited conditions. Flavonoid biosynthesis (bin 16.8) was induced by Fe-stress and persisted unchanged under eCO_2 conditions. Proteins related to stress response (bin 20.1) were upregulated by eCO_2, Fe-limitation, and interaction of eCO_2 with Fe-limitation. Furthermore, several heat-shock proteins (bin 20.2.1) were downregulated by Fe-limitation. Glutathione S-transferases (bin 26.9) and peroxidases (bin 26.12) were upregulated by Fe-limitation and not affected by eCO_2. In addition, several enzymes involved in protein synthesis (bin 29) had lower expression levels at eCO_2 under Fe-sufficient and Fe-limited conditions. Cysteine protease degradation (bin 29.5.3) was upregulated by Fe-limitation and by the interaction of eCO_2 and Fe-limitation.

Table 3. Pathway enrichment analysis in leaves of soybean plants under eCO_2 and Fe-limitation.

Bin Code	Bin Name	Fe+ELE vs. Fe+AMB	*p*-Value	Fe-AMB vs. Fe+AMB	*p*-Value	Fe-ELE vs. Fe+AMB	*p*-Value	Fe-ELE vs. Fe-AMB	*p*-Value
1.1.1	PS. Light reaction. Photosystem II	-	-	DOWN	1.9×10^{-4}	-	-	-	-
1.1.4	PS. Light reaction. Photosystem I	-	-	DOWN	3.0×10^{-2}	-	-	-	-
2.1	Major CHO metabolism. Synthesis	-	-	DOWN	1.0×10^{-2}	-	-	UP	1.2×10^{-4}
3.4	Minor CHO metabolism. Myo-inositol	-	-	-	-	-	-	UP	2.0×10^{-2}
4.1	Glycolysis. Cytosolic branch	UP	2.0×10^{-3}	-	-	-	-	UP	2.0×10^{-2}
11.9.3.3	Lipid metabolism. Lipid degradation. Lysophospholipases. Glycerophosphodiester phosphodiesterase	-	-	DOWN	1.7×10^{-3}	-	-	UP	3.5×10^{-3}
13.2.4	Amino acid metabolism. Degradation. Branched chain	-	-	UP	3.3×10^{-2}	-	-	-	-
16.8	Secondary metabolism. Flavonoids	-	-	UP	6.1×10^{-4}	-	-	-	-
20.1	Stress. Biotic	UP	6.1×10^{-3}	UP	3.7×10^{-4}	UP	1.6×10^{-7}	-	-
20.2.1	Stress. Abiotic. Heat	-	-	DOWN	2.7×10^{-3}	-	-	-	-
26.9	Misc. Glutathione S-transferases	-	-	UP	3.8×10^{-2}	-	-	-	-
26.12	Misc. Peroxidases	-	-	UP	1.3×10^{-4}	UP	1.8×10^{-5}	-	-
28.1.3	DNA. Synthesis/chromatin structure. Histone	DOWN	1.5×10^{-2}	UP	4.1×10^{-2}	-	-	DOWN	2.4×10^{-2}
29.2.1	Protein. Synthesis. Ribosomal protein	DOWN	2.8×10^{-14}	UP	1.9×10^{-13}	-	-	DOWN	9.5×10^{-14}
29.2.2	Protein. Synthesis. Ribosome biogenesis	DOWN	9.8×10^{-3}	-	-	-	-	DOWN	3.8×10^{-3}
29.3.4	Protein. Targeting. Secretory pathway	-	-	-	-	-	-	DOWN	2.8×10^{-3}
29.5.1	Protein. Degradation. Subtilases	-	-	-	-	-	-	UP	2.3×10^{-3}
29.5.3	Protein. Degradation. Cysteine protease	-	-	UP	2.5×10^{-3}	UP	4.1×10^{-3}	-	-
30.5	Signaling. G-proteins	-	-	-	-	DOWN	4.2×10^{-2}	-	-
33.1	Development. Storage proteins	UP	6.5×10^{-6}	UP	8.3×10^{-3}	-	-	DOWN	1.4×10^{-2}
34.9	Transport. Metabolite transporters at the mitochondrial membrane	DOWN	7.8×10^{-3}	-	-	-	-	-	-

3. Discussion

To cope with Fe-stress and eCO_2, soybean plants have evolved complex signaling and metabolic processes at the cellular, organ, and whole-plant levels. Elevated CO_2 promoted plant growth under Fe-sufficient and Fe-limited conditions, as shown in Table 1. Similarly, this "fertilization effect" was reported in tomato [5] and barley plants [13] grown under low levels of Fe supply and eCO_2. However, plant growth decreased under Fe-limitation, particularly at aCO_2, suggesting that eCO_2 could mitigate the Fe deficiency responses. Moreover, Pn was not affected by eCO_2 but reduced in Fe-limited plants promoting leaf chlorosis (Table 1). The statistical analysis also revealed a significant interaction between eCO_2 and Fe-stress on plant growth but not in Pn. Elevated CO_2 significantly increased the sugar content in root and leaf tissues (Table 1). At eCO_2, plants might surpass what they are capable of, using or distributing to sinks, increasing the

carbohydrate content and possibly leading to feedback inhibition of photosynthesis [17]. Sugars are recognized to crosstalk with hormones acting on gene regulation and therefore modify nutrient uptake and transport, among other functions [17]. Lin et al. [18] suggested that sucrose acts as a signaling molecule, causing an increase in auxin and a subsequent increase in nitric oxide, leading to the FIT-mediated transcriptional regulation of FRO2 and IRT1 genes inducing Fe-uptake mechanisms. Although physiological aspects of soybean responses to eCO_2 or Fe-limitation are well studied, proteomic profiling helps understand the molecular basis of soybean adaptation to the upcoming changing climate. Thus, several DEPs were found, in root and leaf tissues, due to eCO_2 and Fe-limitation (Figures 1 and 4). Exposure to eCO_2 and Fe-stress leads to changes in the expression of genes involved in the carbon metabolism in soybean seedlings, especially the expression of genes related to glycolysis, starch and sucrose metabolism, and Myo-inositol metabolism. Elevated CO_2 under Fe-limited conditions stimulated starch and sucrose biosynthesis. Therefore, protein abundance of most enzymes involved in starch (e.g., starch synthase, granule-bound starch synthase, starch-branching enzyme, and 1,4-alpha-glucan branching enzyme) and sucrose biosynthesis (e.g., sucrose-phosphate synthase), were upregulated by eCO_2 conditions (Table 3). The central role of glycolysis is to break down glucose, produce ATP and generate precursors such as fatty acids and amino acids for anabolism [19]. Enzymes involved in glycolysis, such as enolase, pyruvate kinase, phosphofructokinase, glyceraldehyde-3-phosphate dehydrogenase, and phosphoglucomutase, were upregulated by eCO_2 under Fe-limited conditions (Figure S3). Together, these findings led us to suppose that increased energy production via carbohydrate metabolism maintains energy homeostasis. Therefore, eCO_2 increased the transcript levels of genes encoding enzymes involved in foliar cellular respiration, suggesting an improved flux through glycolysis driven by higher carbohydrate bioavailability (starch and sucrose) at eCO_2. Ainsworth et al. [20] also found that growth at eCO_2 led to the stimulation of foliar respiration in soybean plants. This adaptive balance enables plant growth even in the case of Fe-limitation.

In the present study, we found evidence of photosynthesis-related genes in roots (Table 2). DEPs enriched in photosynthesis were upregulated by Fe-limitation and by the interaction of eCO_2 with Fe-limitation. Similarly, Kobayashi et al. [21] reported increased levels of transcription factors responsible for the coordinated expression of genes in chloroplast biogenesis in the roots of *Arabidopsis thaliana*. Accumulation of two golden-2-like transcription factors known to improve phototrophic performance and increase photosynthesis-related proteins in wheat roots under Fe deficiency was reported by Kaur et al. [22]. We hypothesize that this might be a strategy to cope with Fe-stress, thereby increasing CO_2 fixation and demonstrating the possibility of root photosynthesis to improve plants' carbon utilization. In leaves, consistent with protein expression levels, Fe-limitation depressed leaf photosynthesis, which agrees with other studies [4,23–25]. The Fe-AMB treatment produced a higher reduction in plant biomass when compared to the Fe-ELE treatment (Table 1). These results indicated that eCO_2, particularly under Fe-limitation, increased the accumulation of photoassimilates due to eCO_2-induced sugar metabolic pathways. This process is stimulated during adaptation to eCO_2 to generate energy used to maintain leaf growth.

We found many genes involved in flavonoid biosynthesis upregulated after exposure to Fe-stress in leaves and some downregulated in soybean roots. The modulation of genes involved in the biosynthesis of flavonoids suggests that secondary metabolism also plays a role in Fe-stress responses. Several studies reported the effect of various stresses on secondary metabolism in plants [26,27]. Flavonoids are secondary plant products that are biologically active and perform different functions in plants as defense mechanisms against abiotic and biotic stresses [28]. Ahmed et al. [29] demonstrated that drought stress induced the expression of flavonoid biosynthesis genes in hybrid poplar plants and increased the accumulation of phenolic and flavonoid compounds with antioxidant activity. Iron deficiency also increased the expression of crucial enzymes in the flavonoid pathway in *Arabidopsis thaliana* roots [30]. Anyway, the emission of phenolic complexes into the rhizosphere,

involved in Fe deficiency-induced responses, is considered a component of the strategy I plants. It was demonstrated in Arabidopsis roots that coumarins participate in Fe-chelation under Fe deficiency [31]. We found overexpression of feruloyl-CoA 6′-hydroxylase and coumarin synthase involved in coumarin biosynthesis under Fe-limitation in root tissues (Table S3). The above results reinforced the role of coumarins in plant responses to Fe-stress. Table 2 also reveals that a considerable fraction of the carbon flowing through the glycolysis pathway is diverted to secondary metabolism, particularly flavonoid and isoprenoid biosynthesis, which increased at eCO_2 under Fe-limited conditions in root tissues. Under Fe-stress, most proteins included in lignin biosynthesis, such as phenylalanine ammonia-lyase and peroxidase, were downregulated in the roots of soybean plants. Lignin provides mechanical strength to the plant's secondary cell walls, which protect cells from abiotic stresses and serve as the structures that first perceive and respond to environmental stresses. Hence, the downregulation of phenylpropanoid biosynthesis (Figure S4) could save carbon and energy for other metabolic processes [32].

The capacity of cellular redox regulation is crucial to maintaining the activity of many physiological processes [33]. Oxidative stress is often neutralized by enzymatic and non-enzymatic antioxidative systems [34]. The expression of glutathione S-transferase proteins was higher in soybean plants exposed to Fe-limitation (Tables 2 and 3). Glutathione S-transferases are involved in several plant functions as detoxification of xenobiotics, secondary metabolism, growth and development, tetrapyrrole metabolism, and against biotic and abiotic stresses [35,36]. Höhner et al. [37] showed that Fe deficiency increased the expression levels of glutathione S-transferases in *Chlamydomonas reinhardtii*. Similarly, Fe deficiency-induced changes in the protein profile of Arabidopsis thaliana roots and glutathione S-transferases were considered highly expressed proteins [30]. Moreover, the interaction of eCO_2 and Fe-limitation induced the ascorbate-glutathione pathway in roots. Among the antioxidant defense mechanisms, the ascorbate-glutathione pathway is crucial in mitigating further damage to soybean plants caused by reactive oxygen species and derivatives produced during metabolic activity.

Plant growth and development occur due to the global balance between protein synthesis and degradation [33]. Our proteomic analysis showed that many enzymes involved in protein synthesis were downregulated by eCO_2, under Fe-sufficient and Fe-limited conditions, in root and leaf tissues. These results could be associated with the fact that increased levels of carbohydrates can affect gene expression through their role as signaling molecules. Sugars could be involved in photosynthetic acclimation, whereby the additional carbohydrates formed under eCO_2 conditions might cause the downregulation of photosynthetic gene transcripts and suppress protein synthesis [17]. However, photosynthetic acclimation does not always completely negate the positive results eCO_2 has on plant growth. The positive effects of eCO_2 on plant growth are well studied, but the role of hormone pathways in regulating the growth responses under eCO_2 is slightly understood. Gibberellins are a class of diterpenoid hormones involved in several growths and developmental processes, including stem elongation, leaf expansion, flower development, and germination [38]. Biosynthesis of gibberellins includes 2-oxoglutarate/Fe(II)-dependent dioxygenases that are upregulated at eCO_2, under Fe-limited and Fe-sufficient conditions, in this study. An increase in gibberellins expression under eCO_2 has also been reported in species such as *Ginkgo biloba* [39], *Arabidopsis thaliana* [40], and *Populus tomentosa* [41]. Our finding suggests that eCO_2 might play a role in signaling, allowing higher plant growth rates.

Most enzymes involved in the stress responses, including heat-shock proteins, had low expression levels under Fe-limitation in soybean plants. The role of heat-shock proteins is to manage protein folding and promote cellular protection, protein homeostasis, and cell survival against several environmental and metabolic stresses [14,42]. We infer that soybean plants had lower levels of protein structure protection under Fe-limited conditions. In addition, proteins involved in cell-wall organization, including UDP-glucose 6-dehydrogenase, cellulose synthase, and xyloglucan endotransglucosylase, were downregulated by Fe-stress and by the interaction of eCO_2 with Fe-stress in root tissues (Table S3). The reduced level

of cell wall-modifying genes could limit cell expansion as plant growth decreased under Fe-limitation. The extent and severity of abiotic stresses or the crops selected are crucial in determining the effects of eCO_2 and Fe-stress. Therefore, eCO_2 and Fe-stress influence the growth and yield of plants and their subsequent adaptation to future climate changes and should require more attention from the scientific community.

4. Materials and Methods

4.1. Plant Material and Growth Conditions

A previously identified highly-CO_2 responsive soybean variety Wisconsin Black [43], was used as plant material. This study was performed at the Biotechnology School of Catholica University (Portugal). Plants were grown under hydroponic conditions in black plastic pots (5 L) filled with an aerated, full-strength nutrient solution with the following composition: 1.2 mM KNO_3, 0.8 mM $Ca(NO_3)_2$, 0.3 mM $MgSO_4.7H_2O$, 0.2 mM $NH_4H_2PO_4$, 25 µM $CaCl_2$, 25 µM H_3BO_3, 0.5 µM $MnSO_4$, 2 µM $ZnSO_4.H_2O$, 0.5 µM $CuSO_4.H_2O$, 0.5 µM MoO_3, 0.1 µM $NiSO_4$, and 20 µM Fe(III)-EDDHA. The solution was buffered by MES (1mM, pH 5.5) addition and changed every 3 d. The growth chamber was controlled to maintain the temperature at 25 °C (day period) and 20 °C (dark period), relative humidity at 75 %, and photosynthetic photon flux density at 325 µmol s^{-1} m^{-2} (daytime light). After 7 days of pre-treatment in the complete nutrient solution under aCO_2, plants were transferred to a nutrient solution with Fe(III)-EDDHA at 0.5 µM (Fe-limited) or 20 µM (Fe-sufficient). Then, half of the plants were grown at 400 ppm (aCO_2), and the other half were grown at 800 ppm (eCO_2) in independent growth chambers for 12 days. The CO_2 concentration was continuously monitored and maintained by an automated CO_2 control system, which measured and adjusted the CO_2 concentration from soybean planting to the end of the experiment.

4.2. Evaluation of Plant Biomass

At the end of the experiment, plants were dried in an oven at 70 ºC until constant weight for total plant biomass determination.

4.3. Leaf Gas Exchange Parameters

Leaf gas exchange measurements were performed on day 17 after the beginning of the experiment. We randomly selected the first expanded trifoliate leaf from 3 plants (n = 9), and the photosynthetic rate was measured using a portable photosynthesis system (LI-6400XT; LI-COR, Lincoln, NE, USA). The CO_2 in the leaf chamber was set to match the CO_2 treatment, with a photosynthetic photon flux density of 500 µmol photon m^{-2} s^{-1} at 25 °C. Moreover, the transpiration rate and stomatal conductance were determined.

4.4. Root and Leaf Carbohydrates

Root and leaf samples (n = 5) were evaluated for carbohydrate analysis at the end of the experiment. The extraction protocol was described by López-Millán et al. [44]. About 100 mg of plant material was grounded using liquid nitrogen, suspended in 5 mM H2SO4, vortexed for 30 s, and then boiled for 30 min. Samples were centrifuged at 2320× g for 10 min, supernatant was filtered through a 0.45 mm PTFE filter, and the volume was adjusted to 2 mL and stored at −80 °C until further analysis. The HPLC system consisted of an ion exchange aminex HPX-87H Column (Bio-Rad, Hercules, CA, USA) maintained at 40 °C. The mobile phase was 5 mM H_2SO_4 at a flow rate of 0.6 mL min^{-1}.

4.5. Protein Extraction and LC−MS/MS Analysis

The protein extraction was based on the protocol developed by Wu et al. [45]. We used three biological replicates to perform the proteome analysis. From each sample, 250 mg of frozen plant tissue was ground in liquid nitrogen. The powdered tissue was dissolved in cold acetone (−20 °C) with TCA (10% wt/vol), homogenized with acid-washed sand, and centrifuged at 15,000× g for 5 min at 4 °C to collect the precipitated proteins. The

pellet was resuspended in cold TCA/acetone, vortexed, and centrifuged at 15,000× *g* for 5 min at 4 °C to collect proteins and repeated until the pellet turned white. Then, the pellet was resuspended twice in 1.5 mL of cold acetone, centrifuged at 15,000g for 5 min at 4 °C, and the supernatant was discarded. Next, the pellet was air-dried in a fume hood and resuspended in an SDS extraction buffer for 1.5 h. Then, centrifuged at 15,000× *g* for 10 min, the supernatant was collected into new Eppendorf tubes, mixed with an equal volume of Tris-buffered phenol, and vortexed for 3 min. The mixture was centrifuged at 15,000× *g* for 5 min, and the lower phenol phase was collected into a new Eppendorf tube. An equal volume of washing buffer I was added to the phenol phase, vortexed by 3 min, and centrifuged at 15,000× *g* for 5 min at room temperature. The upper phase (phenol phase) was collected into a new Eppendorf tube, and 0.1 M ammonium acetate in methanol was added to a final volume of 2.0 mL. The mixture was vortexed for 30 s and stored at −20 °C for 2 h to precipitate the phenol-extracted proteins. The solution was centrifuged at 15,000× *g* for 10 min at 4 °C, and the supernatant was discarded. The protein pellets were resuspended with 0.1 M ammonium acetate in methanol and centrifuged at 15,000× *g* for 5 min at 4 °C, and the supernatant was rejected. Therefore, the pellets were resuspended in 80% (*v*/*v*) acetone, centrifuged at 15,000× *g* for 5 min at 4 °C, and the supernatant was removed. The protein pellets were air-dried at room temperature and resuspended in 100 µL of rehydration buffer (50 mM ammonium carbonate, 8 M urea). The concentrations of the protein extracts were determined by the Bradford assay [46].

Each sample was processed for proteomic analysis following the solid-phase-enhanced sample-preparation (SP3) protocol and enzymatically digested with Trypsin/LysC as previously described [47]. Protein identification and quantitation were performed by nanoLC-MS/MS following an already published procedure [48] using a nanoLC flow rate of 300 nL/min. For protein identification and quantification, the UniProt database was considered for the Glycine max Proteome (2020_01). The proteomics data analysis was performed with the Proteome Discoverer 2.4.0.305 software (Thermo Scientific, San Jose, CA, USA.

4.6. Database Search and Protein Quantification

Only high-confidence peptides and proteins with at least two unique peptides detected in all three replicates were used in quantification. For all quantified proteins, only those showing a fold change of above 1.2 or below 1/1.2 (for the mean of the three replicates) in the quantitative ratios and $p < 0.05$ were considered as differentially expressed proteins (DEPs). Protein sequences were submitted to the online Mercator 4 annotation tool [49] for proteome annotation. Protein functions were categorized using Mapman bin codes, and the protein abundance ratio was visualized through MapMan software [50]. Pathway enrichment analysis of DEPs was performed using Fisher's exact test. Information about the subcellular location was accomplished from the location available from SUBA4 [51].

4.7. Statistical Analysis

Data were analyzed using SPSS software (SPSS version 26.0). Analysis of variance (2way ANOVA) was used to determine differences among different treatments after data normality and equal variance analysis. The means ± SE were calculated for each parameter.

5. Conclusions

Elevated CO_2 and Fe-stress had profound effects on plant biomass, sugar content, and Pn, with interactive effects of eCO_2 and Fe-stress on plant biomass. Overall, the CO_2-induced increase in biomass was not significantly different between Fe+ELE and Fe-ELE treatments. We performed proteomic analysis to analyze DEPs affected by the interaction of Fe-limitation and eCO_2 in soybean plants. Overall, root and leaf tissues contained 705 and 589 DEPs, respectively. Based on pathway enrichment analysis, cell wall organization, glutathione metabolism, photosynthesis, stress-related proteins, and biosynthesis of secondary compounds changed in roots to cope with Fe-stress. Moreover,

the enhanced plant growth by eCO_2 supplied with sufficient or insufficient Fe was associated with the increased abundance of proteins involved in glycolysis, starch and sucrose metabolism, biosynthesis of gibberellins, and decreased levels of protein biosynthesis. The understanding of plant productivity and adaptation to future climate changes will also improve through future studies created to compare responses across various cultivars and during different periods of stress exposure.

Supplementary Materials: The supporting information can be downloaded at: https://www.mdpi.com/article/10.3390/ijms232113632/s1.

Author Contributions: Conceptualization, J.C.S.; methodology, J.C.S. and H.O.; software, J.C.S. and H.O.; validation, M.W.V.; investigation, J.C.S. and H.O.; writing—original draft preparation, J.C.S.; writing—review and editing, M.W.V. and M.P.; supervision, M.W.V.; project administration, M.W.V.; funding acquisition, J.C.S. and M.W.V. All authors have read and agreed to the published version of the manuscript.

Funding: This research was funded by National Funds from FCT—Fundação para a Ciência e Tecnologia through project UIDB/50016/2020 and by FCT project PTDC/AGR-PRO/3972/2014. This work was also financed by the Portuguese Mass Spectrometry Network, integrated in the National Roadmap of Research Infrastructures of Strategic Relevance (ROTEIRO/0028/2013; LISBOA-01-0145-FEDER-022125). The authors gratefully acknowledge the International Ph.D. Program in Biotechnology, Portugal, for providing Ph.D. scholarship (No. NORTE-08-5369-FSE-000007) to José Carvalho Soares.

Institutional Review Board Statement: Not applicable.

Informed Consent Statement: Not applicable.

Data Availability Statement: The data presented in this study are available in the supplementary material.

Conflicts of Interest: The authors declare no conflict of interest.

References

1. Meehl, G.A.; Washington, W.M.; Santer, B.D.; Collins, W.D.; Arblaster, J.M.; Hu, A.; Lawrence, D.M.; Teng, H.; Buja, L.E.; Strand, W.G. Climate Change Projections for the Twenty-First Century and Climate Change Commitment in the CCSM3. *J. Clim.* **2006**, *19*, 2597–2616. [CrossRef]
2. Yu, J.; Fan, N.; Li, R.; Zhuang, L.; Xu, Q.; Huang, B. Proteomic Profiling for Metabolic Pathways Involved in Interactive Effects of Elevated Carbon Dioxide and Nitrogen on Leaf Growth in a Perennial Grass Species. *J. Proteome Res.* **2019**, *18*, 2446–2457. [CrossRef]
3. Zheng, G.; Chen, J.; Li, W. Impacts of CO2 elevation on the physiology and seed quality of soybean. *Plant Divers.* **2020**, *42*, 44–51. [CrossRef]
4. Briat, J.-F.; Dubos, C.; Gaymard, F. Iron nutrition, biomass production, and plant product quality. *Trends Plant Sci.* **2015**, *20*, 33–40. [CrossRef] [PubMed]
5. Jin, C.W.; Du, S.T.; Chen, W.W.; Li, G.X.; Zhang, Y.S.; Zheng, S.J. Elevated Carbon Dioxide Improves Plant Iron Nutrition through Enhancing the Iron-Deficiency-Induced Responses under Iron-Limited Conditions in Tomato. *Plant Physiol.* **2009**, *150*, 272–280. [CrossRef] [PubMed]
6. Jin, C.W.; Liu, Y.; Mao, Q.Q.; Wang, Q.; Du, S.T. Mild Fe-deficiency improves biomass production and quality of hydroponic-cultivated spinach plants (*Spinacia oleracea* L.). *Food Chem.* **2013**, *138*, 2188–2194. [CrossRef]
7. Takahashi, M.; Nakanishi, H.; Kawasaki, S.; Nishizawa, N.K.; Mori, S. Enhanced tolerance of rice to low iron availability in alkaline soils using barley nicotianamine aminotransferase genes. *Nat. Biotechnol.* **2001**, *19*, 466–469. [CrossRef]
8. Myers, S.S.; Zanobetti, A.; Kloog, I.; Huybers, P.; Leakey, A.D.B.; Bloom, A.J.; Carlisle, E.; Dietterich, L.H.; Fitzgerald, G.; Hasegawa, T.; et al. Increasing CO2 threatens human nutrition. *Nature* **2014**, *510*, 139–142. [CrossRef]
9. Burgess, P.; Huang, B. Leaf protein abundance associated with improved drought tolerance by elevated carbon dioxide in creeping bentgrass. *J. Am. Soc. Hortic. Sci.* **2016**, *141*, 85–96. [CrossRef]
10. Burgess, P.; Huang, B. Root protein metabolism in association with improved root growth and drought tolerance by elevated carbon dioxide in creeping bentgrass. *Field Crops Res.* **2014**, *165*, 80–91. [CrossRef]
11. Yu, J.; Li, R.; Fan, N.; Yang, Z.; Huang, B. Metabolic pathways involved in carbon dioxide enhanced heat tolerance in bermudagrass. *Front. Plant Sci.* **2017**, *8*, 1506. [CrossRef] [PubMed]
12. Robin, A.; Vansuyt, G.; Hinsinger, P.; Meyer, J.M.; Briat, J.F.; Lemanceau, P. Chapter 4 Iron Dynamics in the Rhizosphere: Consequences for Plant Health and Nutrition. In *Advances in Agronomy*; Academic Press: Cambridge, MA, USA, 2008; Volume 99, pp. 183–225.

13. Haase, S.; Rothe, A.; Kania, A.; Wasaki, J.; Römheld, V.; Engels, C.; Kandeler, E.; Neumann, G. Responses to Iron Limitation in Hordeum vulgare L. as Affected by the Atmospheric CO_2 Concentration. *J. Environ. Qual.* **2008**, *37*, 1254–1262. [CrossRef] [PubMed]
14. Donnini, S.; Prinsi, B.; Negri, A.S.; Vigani, G.; Espen, L.; Zocchi, G. Proteomic characterization of iron deficiency responses in Cucumis sativus L. roots. *BMC Plant Biol.* **2010**, *10*, 1–15. [CrossRef] [PubMed]
15. Meisrimler, C.-N.; Wienkoop, S.; Lyon, D.; Geilfus, C.-M.; Lüthje, S. Long-term iron deficiency: Tracing changes in the proteome of different pea (Pisum sativum L.) cultivars. *J. Proteom.* **2016**, *140*, 13–23. [CrossRef]
16. López-Millán, A.-F.; Grusak, M.; Abadia, A.; Abadía, J. Iron deficiency in plants: An insight from proteomic approaches. *Front. Plant Sci.* **2013**, *4*, 254. [CrossRef]
17. Thompson, M.; Gamage, D.; Hirotsu, N.; Martin, A.; Seneweera, S. Effects of Elevated Carbon Dioxide on Photosynthesis and Carbon Partitioning: A Perspective on Root Sugar Sensing and Hormonal Crosstalk. *Front. Physiol.* **2017**, *578*, 1–13. [CrossRef]
18. Lin, X.Y.; Ye, Y.Q.; Fan, S.K.; Jin, C.W.; Zheng, S.J. Increased Sucrose Accumulation Regulates Iron-Deficiency Responses by Promoting Auxin Signaling in Arabidopsis Plants. *Plant Physiol.* **2016**, *170*, 907–920. [CrossRef]
19. Chen, T.; Zhang, L.; Shang, H.; Liu, S.; Peng, J.; Gong, W.; Shi, Y.; Zhang, S.; Li, J.; Gong, J. iTRAQ-based quantitative proteomic analysis of cotton roots and leaves reveals pathways associated with salt stress. *PLoS ONE* **2016**, *11*, e0148487. [CrossRef]
20. Ainsworth, E.A.; Rogers, A.; Vodkin, L.O.; Walter, A.; Schurr, U. The Effects of Elevated CO_2 Concentration on Soybean Gene Expression. An Analysis of Growing and Mature Leaves. *Plant Physiol.* **2006**, *142*, 135–147. [CrossRef]
21. Kobayashi, K.; Baba, S.; Obayashi, T.; Sato, M.; Toyooka, K.; Keränen, M.; Aro, E.M.; Fukaki, H.; Ohta, H.; Sugimoto, K.; et al. Regulation of root greening by light and auxin/cytokinin signaling in Arabidopsis. *Plant Cell* **2012**, *24*, 1081–1095. [CrossRef]
22. Kaur, G.; Shukla, V.; Kumar, A.; Kaur, M.; Goel, P.; Singh, P.; Shukla, A.; Meena, V.; Kaur, J.; Singh, J.; et al. Integrative analysis of hexaploid wheat roots identifies signature components during iron starvation. *J. Exp. Bot.* **2019**, *70*, 6141–6161. [CrossRef] [PubMed]
23. Jiang, C.D.; Gao, H.Y.; Zou, Q.; Shi, L. Effects of iron deficiency on photosynthesis and photosystem II function in soybean leaf. *J. Plant Physiol. Mol. Biol.* **2007**, *33*, 53–60.
24. Therby-Vale, R.; Lacombe, B.; Rhee, S.Y.; Nussaume, L.; Rouached, H. Mineral nutrient signaling controls photosynthesis: Focus on iron deficiency-induced chlorosis. *Trends Plant Sci.* **2021**, *27*, 502–509. [CrossRef] [PubMed]
25. Andaluz, S.; López-Millán, A.-F.; De las Rivas, J.; Aro, E.-M.; Abadía, J.; Abadía, A. Proteomic profiles of thylakoid membranes and changes in response to iron deficiency. *Photosynth. Res.* **2006**, *89*, 141–155. [CrossRef] [PubMed]
26. Austen, N.; Walker, H.J.; Lake, J.A.; Phoenix, G.K.; Cameron, D.D. The Regulation of Plant Secondary Metabolism in Response to Abiotic Stress: Interactions Between Heat Shock and Elevated CO_2. *Front. Plant Sci.* **2019**, *10*, 1463. [CrossRef]
27. Ramakrishna, A.; Ravishankar, G.A. Influence of abiotic stress signals on secondary metabolites in plants. *Plant Signal. Behav.* **2011**, *6*, 1720–1731. [CrossRef]
28. Falcone Ferreyra, M.L.; Rius, S.; Casati, P. Flavonoids: Biosynthesis, biological functions, and biotechnological applications. *Front. Plant Sci.* **2012**, *3*, 222. [CrossRef]
29. Ahmed, U.; Rao, M.J.; Qi, C.; Xie, Q.; Noushahi, H.A.; Yaseen, M.; Shi, X.; Zheng, B. Expression Profiling of Flavonoid Biosynthesis Genes and Secondary Metabolites Accumulation in Populus under Drought Stress. *Molecules* **2021**, *26*, 5546. [CrossRef]
30. Lan, P.; Li, W.; Wen, T.N.; Shiau, J.Y.; Wu, Y.C.; Lin, W.; Schmidt, W. iTRAQ protein profile analysis of Arabidopsis roots reveals new aspects critical for iron homeostasis. *Plant Physiol.* **2011**, *155*, 821–834. [CrossRef]
31. Perkowska, I.; Potrykus, M.; Siwinska, J.; Siudem, D.; Lojkowska, E.; Ihnatowicz, A. Interplay between Coumarin Accumulation, Iron Deficiency and Plant Resistance to *Dickeya* spp. *Int. J. Mol. Sci.* **2021**, *22*, 6449. [CrossRef]
32. Jia, X.-m.; Zhu, Y.-f.; Hu, Y.; Zhang, R.; Cheng, L.; Zhu, Z.-l.; Zhao, T.; Zhang, X.; Wang, Y.-x. Integrated physiologic, proteomic, and metabolomic analyses of Malus halliana adaptation to saline–alkali stress. *Hortic. Res.* **2019**, *6*, 91. [CrossRef] [PubMed]
33. Zhang, X.; Högy, P.; Wu, X.; Schmid, I.; Wang, X.; Schulze, W.X.; Jiang, D.; Fangmeier, A. Physiological and proteomic evidence for the interactive effects of post-anthesis heat stress and elevated CO2 on wheat. *Proteomics* **2018**, *18*, 1800262. [CrossRef] [PubMed]
34. Kapoor, D.; Singh, S.; Kumar, V.; Romero, R.; Prasad, R.; Singh, J. Antioxidant enzymes regulation in plants in reference to reactive oxygen species (ROS) and reactive nitrogen species (RNS). *Plant Gene* **2019**, *19*, 100182. [CrossRef]
35. Dalton, D.A.; Boniface, C.; Turner, Z.; Lindahl, A.; Kim, H.J.; Jelinek, L.; Govindarajulu, M.; Finger, R.E.; Taylor, C.G. Physiological roles of glutathione S-transferases in soybean root nodules. *Plant Physiol.* **2009**, *150*, 521–530. [CrossRef]
36. Vaish, S.; Gupta, D.; Mehrotra, R.; Mehrotra, S.; Basantani, M.K. Glutathione S-transferase: A versatile protein family. *3 Biotech.* **2020**, *10*, 321. [CrossRef]
37. Höhner, R.; Barth, J.; Magneschi, L.; Jaeger, D.; Niehues, A.; Bald, T.; Grossman, A.; Fufezan, C.; Hippler, M. The metabolic status drives acclimation of iron deficiency responses in Chlamydomonas reinhardtii as revealed by proteomics based hierarchical clustering and reverse genetics. *Mol. Cell. Proteom.* **2013**, *12*, 2774–2790. [CrossRef]
38. Ribeiro, D.M.; Araújo, W.L.; Fernie, A.R.; Schippers, J.H.; Mueller-Roeber, B. Action of gibberellins on growth and metabolism of Arabidopsis plants associated with high concentration of carbon dioxide. *Plant Physiol.* **2012**, *160*, 1781–1794. [CrossRef]
39. Li, C.R.; Gan, L.J.; Xia, K.; Zhou, X.; Hew, C.S. Responses of carboxylating enzymes, sucrose metabolizing enzymes and plant hormones in a tropical epiphytic CAM orchid to CO_2 enrichment. *Plant Cell Environ.* **2002**, *25*, 369–377. [CrossRef]
40. Teng, N.; Wang, J.; Chen, T.; Wu, X.; Wang, Y.; Lin, J. Elevated CO_2 induces physiological, biochemical and structural changes in leaves of Arabidopsis thaliana. *New Phytol.* **2006**, *172*, 92–103. [CrossRef]

41. Liu, J.; Zhang, J.; He, C.; Duan, A. Genes responsive to elevated CO_2 concentrations in triploid white poplar and integrated gene network analysis. *PLoS ONE* **2014**, *9*, e0098300. [CrossRef]
42. Bai, J.; Jin, K.; Qin, W.; Wang, Y.; Yin, Q. Proteomic Responses to Alkali Stress in Oats and the Alleviatory Effects of Exogenous Spermine Application. *Front. Plant Sci.* **2021**, *12*, 627129. [CrossRef] [PubMed]
43. Soares, J.; Deuchande, T.; Valente, L.M.P.; Pintado, M.; Vasconcelos, M.W. Growth and nutritional responses of bean and soybean genotypes to elevated CO_2 in a controlled environment. *Plants* **2019**, *8*, 465. [CrossRef]
44. López-Millán, A.; Morales, F.; Gogorcena, Y.; Abadía, A.; Abadía, J. Metabolic responses in iron deficient tomato plants. *J. Plant Physiol.* **2009**, *166*, 375–384. [CrossRef]
45. Wu, X.; Xiong, E.; Wang, W.; Scali, M.; Cresti, M. Universal sample preparation method integrating trichloroacetic acid/acetone precipitation with phenol extraction for crop proteomic analysis. *Nat. Protoc.* **2014**, *9*, 362–374. [CrossRef] [PubMed]
46. Bradford, M.M. A rapid and sensitive method for the quantitation of microgram quantities of protein utilizing the principle of protein-dye binding. *Anal. Biochem.* **1976**, *72*, 248–254. [CrossRef]
47. Osório, H.; Silva, C.; Ferreira, M.; Gullo, I.; Máximo, V.; Barros, R.; Mendonça, F.; Oliveira, C.; Carneiro, F. Proteomics Analysis of Gastric Cancer Patients with Diabetes Mellitus. *J. Clin. Med.* **2021**, *10*, 407. [CrossRef]
48. Casanova, M.R.; Osório, H.; Reis, R.L.; Martins, A.; Neves, N.M. Chondrogenic differentiation induced by extracellular vesicles bound to a nanofibrous substrate. *NPJ Regen. Med.* **2021**, *6*, 79. [CrossRef]
49. Schwacke, R.; Ponce-Soto, G.Y.; Krause, K.; Bolger, A.M.; Arsova, B.; Hallab, A.; Gruden, K.; Stitt, M.; Bolger, M.E.; Usadel, B. MapMan4: A Refined Protein Classification and Annotation Framework Applicable to Multi-Omics Data Analysis. *Mol. Plant* **2019**, *12*, 879–892. [CrossRef]
50. Thimm, O.; Bläsing, O.; Gibon, Y.; Nagel, A.; Meyer, S.; Krüger, P.; Selbig, J.; Müller, L.A.; Rhee, S.Y.; Stitt, M. mapman: A user-driven tool to display genomics data sets onto diagrams of metabolic pathways and other biological processes. *Plant J.* **2004**, *37*, 914–939. [CrossRef]
51. Hooper, C.M.; Castleden, I.R.; Tanz, S.K.; Aryamanesh, N.; Millar, A.H. SUBA4: The interactive data analysis centre for Arabidopsis subcellular protein locations. *Nucleic Acids Res.* **2017**, *45*, 1064–1074. [CrossRef]